Progress In Electromagnetics Research B, Vol. 80, 101–112, 2018

Fast Calculation and Analysis of the Equivalent Impedance of a Wireless Power Transfer System Using an Array of Magnetically Coupled Resonators

José Alberto[1, *], Ugo Reggiani[1], Leonardo Sandrolini[1], and Helena Albuquerque[2]

Abstract—In this paper the equivalent impedance of resonator arrays for wireless power transfer systems is obtained in closed-form from a continued fraction expression. Using the theory of difference equations, the continued fraction is described as the general term of a complex sequence defined by recurrence, and its convergence is analyzed. It is shown that the equivalent impedance can be easily found in closed-form in terms of the system parameters. In this way, the obtained closed-form expressions may help electrical engineers to quickly predict the behaviour of a system with the changes of its parameters. Some numerical examples of the theoretical results are given and discussed. Finally, the analytical formulae obtained in this work are validated with measurements and a good agreement is observed.

1. INTRODUCTION

Recently, many studies have been focused on wireless power transfer WPT systems to transfer power without electrical contact in several applications [1–3]. In situations of high misalignment or distance between the emitter and receiver coils, the use of intermediate resonators [4–10] can increase the efficiency of these systems and make it possible to transmit power over longer distances. These resonators can be arranged in arrays on a plane with parallel axes, or in a domino configuration. In this way we can build a device capable of charging a small electronic device, or electric vehicle, in several positions along the array (planar array) or be able to charge or power a device at a longer distance (domino array). Usually one of the resonators of the array is connected to the power source and transmits power through magnetic coupling to a load connected at the other end of the array or to one or more receivers over the array.

Magnetoinductive wave theory (MIW) has been used to study these arrays [11, 12], which can also be analysed using a circuit modelling approach: after removing the resonator of the array connected to the source, the rest of the array can be described with an equivalent impedance. This equivalent impedance allows one to analyse the power delivered by the source to the loaded array (the array facing a receiver or terminated in a load, i.e., using the last resonator of the line as receiver), to examine impedance matching of the source to the loaded resonator array and can be useful for the design of the array and its power source.

This equivalent impedance is described as a continued fraction in [11, 13]. Continued fractions play an important role in a variety of branches of applied sciences, as in [14, 15]. Although in [11] it is simply acknowledged that an analytical study of this fraction seems not to be possible, in this paper, by performing a mathematical study of the continued fraction as the general term of a complex

Received 17 January 2018, Accepted 27 March 2018, Scheduled 10 April 2018

* Corresponding author: José Alberto (jose.mamede2@unibo.it).

[1] Department of Electrical, Electronic, and Information Engineering, University of Bologna, Viale del Risorgimento 2, I-40136 Bologna, Italy. [2] Department of Mathematics of University of Coimbra, Coimbra, Portugal.

sequence defined by recurrence, we obtain a closed-form expression of the equivalent impedance for any condition of the system. The general term of the recursive sequence is determined through the resolution of a linear homogeneous difference equation with constant coefficients and its value can then be calculated just knowing the initial conditions and possible perturbations on the system. Through the closed-form expressions, a better insight of the behaviour of the system with respect to the variation of its geometrical and electrical parameters can be achieved. Indeed, the results of this paper are useful for electrical engineers in the design of a WPT system using an array of resonators, especially regarding impedance matching and the design of the power source. Therefore, as the analysis is made simpler and faster through the closed-form expressions even for several conditions of the system (different circuit parameters, number of resonators, number receivers), designers can save time and increase the calculation precision compared with using electromagnetic simulation software.

In this paper, a description of the analysed circuit is provided in Section 2. The closed-form expressions for the equivalent impedance of a resonator array with a receiver over the array at the end or at any other position of the array are presented in Section 3, together with a numerical study of their values and convergence. The mathematical approach used to develop these expressions, for simplicity of the presentation, is detailed in the Appendix. Finally, in the last section of this paper experiments are carried out to validate the theoretical results presented in this paper, by measuring both the input impedance and the input power and their variation with the equivalent impedance of the array.

2. DESCRIPTION OF THE CIRCUIT

The system that we consider in this work, as shown in Fig. 1(a), consists of an array of $n+1$ identical resonators (cells) arranged in a plane along a line to form a planar structure; two adjacent resonators are spaced by the same constant distance and are magnetically coupled with a mutual inductance M, whereas the coupling between nonadjacent resonators is neglected, as done also in [5, 11, 13]. Each cell can be described as an R-L-C series circuit, as in [16] where R represents the intrinsic resistance of the cell, L its self-inductance and C the additional capacitance needed to tune the resonant frequency of the cell. The impedance of each cell is then given by $\hat{Z} = R + j\omega L + 1/(j\omega C)$, being $\omega = 2\pi f$ the angular frequency, that becomes $\hat{Z} = R$ at the resonant angular frequency $\omega_0 = 2\pi f_0 = 1/\sqrt{LC}$. The cell of the resonator array connected to a source of sinusoidal voltage $\hat{V}_s$ and internal resistance R_s is labeled $n+1$, whereas the cell at the other end of the line is connected to a termination impedance $\hat{Z}_T$ and labeled 1.

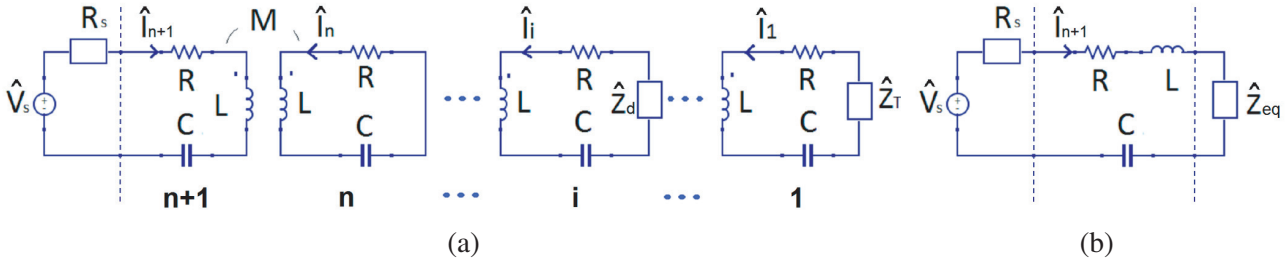

Figure 1. Equivalent circuit of a system composed of $n+1$ cells with (a) the impedance $\hat{Z}_d$ inserted in the ith cell, representing the receiver over it and (b) the same system with an impedance $\hat{Z}_{eq}$ representing the resonator array (removing the resonator connected to the source) and the receiver.

When there is a receiver above the line, the receiver absorbs part of the power arriving from the source at the ith cell under it, with $1 \leq i \leq n$, and this fact represents a perturbation in the system. This perturbation caused by the magnetic coupling between the receiver and the ith cell can be represented by $\hat{Z}_d$, as seen in Fig. 1(a), which is the impedance of the receiver seen from the cell which is under it [11, 13]. It is assumed that the receiver has the same electrical parameters as the cells of the array and, consequently, has the same resonant frequency.

The WPT system can be further simplified by introducing an equivalent impedance $\hat{Z}_{eq}$, that represents the impedance of the array and the receivers after removing the resonator connected to the power source, as depicted in Fig. 1(b). As seen in [13], the equivalent impedance $\hat{Z}_{eq}$ has the following expression when the receiver coil is placed over any cell of the resonator array:

$$\hat{Z}_{eq} = \cfrac{(\omega M)^2}{\hat{Z} + \cfrac{(\omega M)^2}{\ldots + \cfrac{(\omega M)^2}{\hat{Z}_d + \hat{Z} + \cfrac{(\omega M)^2}{\hat{Z} + \cfrac{(\omega M)^2}{\ldots + \cfrac{(\omega M)^2}{\hat{Z} + \cfrac{(\omega M)^2}{\hat{Z} + \hat{Z}_T}}}}}}}. \tag{1}$$

Note that we can replace $\hat{Z}_T$ by $\hat{Z}'_T$ in Eq. (1), in the particular case where the first cell of the resonator array is connected to a load and therefore this cell is the receiver ($\hat{Z}'_T = \hat{Z}_T$) or a receiver is placed over the first cell $\hat{Z}'_T = \hat{Z}_T + \hat{Z}_d$. Moreover, in case we are operating at the resonant angular frequency ω_0, Eq. (1) can be written with $\hat{Z} = R$, $\hat{Z}_T = R_T$, $\hat{Z}_d = R_d$.

The mathematical analysis developed to determine the value of the continued fraction that represents the impedance of an array of resonators is illustrated in the Appendices. It is demonstrated that the fraction can be rewritten as a term of a recursive sequence whose general term can be determined using the theory of linear homogeneous difference equations [17]. In this way, we get an expression for the value of the fraction that depends only on its initial conditions, number of terms and order of the term which is affected by the perturbation. This expression is shown in the next section.

3. CLOSED-FORM EXPRESSIONS OF THE CONTINUED FRACTION

The theoretical results obtained in the Appendices are now applied to a WPT system composed of an array of resonators, and closed-form expressions for Eq. (1), considered for the two cases with $\omega \neq \omega_0$ and $\omega = \omega_0$, are found. Examples of calculations are carried out with the software MATLAB, and some numerical results are presented and discussed. In order to illustrate possible practical situations, the values for R, L, C and M used are the ones obtained through measurements performed with the experimental setup described in Section 4 ($L = 12.6\,\mu\text{H}$, $C = 93.1\,\text{nF}$, $R = 0.11\,\Omega$, $M = -1.55\,\mu\text{H}$ and $f_0 = 147\,\text{kHz}$).

To obtain the expression of the equivalent impedance $\hat{Z}_{eq}$, we write the generic values of the fractions in Eqs. (A7) and (A11) in terms of the characteristics of the WPT system shown in Section 2, $a = (\omega M)^2$, $b = \hat{Z}$, $x_0 = \hat{Z}'_T = \hat{Z}_T + \hat{Z}_d$ (which is reduced to $\hat{Z}_T$ when the receiver is not over the first cell), $b' = \hat{Z}_d + \hat{Z}$.

Equivalent impedance with resonator number 1 acting as receiver or with a receiver over the first cell of the resonator line

$$\hat{Z}_{eq} = \frac{f^n(2(\omega M)^2 - g\hat{Z}'_T) + g^n(f\hat{Z}'_T - 2(\omega M)^2)}{f^n(f + 2\hat{Z}'_T) - g^n(g + 2\hat{Z}'_T)} \tag{2}$$

where $f = \hat{Z} - \sqrt{\hat{Z}^2 + 4(\omega M)^2}$ and $g = \hat{Z} + \sqrt{\hat{Z}^2 + 4(\omega M)^2}$.

Equivalent impedance with a receiver over the resonator line at any position (e.g., over the ith cell)

$$\hat{Z}_{eq} = \frac{(\omega M)^2\left(e_1 f^n g^{2i} + e_2 f^{2i} g^n - f^i g^i\left(e_3 f^n + e_4 g^n\right)\right)}{f^n g^i\left(e_5 f^i + e_6 g^i\right) + f^i g^n\left(e_7 f^i + e_8 g^i\right)} \tag{3}$$

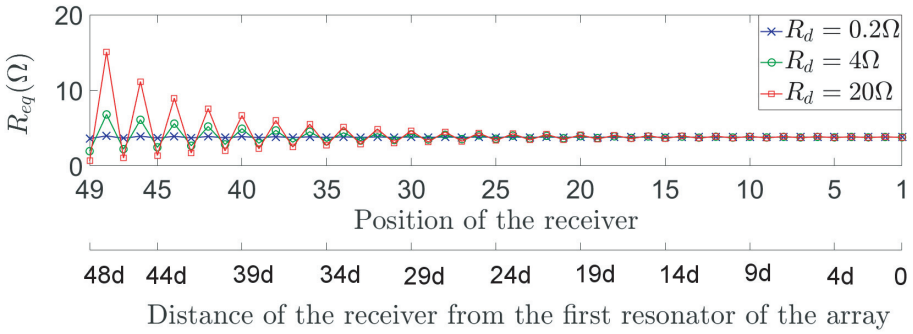

Figure 2. R_{eq} versus the position of the receiver over an array of 50 resonators for different values of R_d, at the resonant frequency $f_0 = 147\,\text{kHz}$ and for $R_T = 1.5\,\Omega$. The position of the receiver is 49 when over the cell next to the one connected to the source and 1 when over the cell at the other end of the array line. The position of the receiver along the longitudinal axis of the array is also represented in terms of the distance d between the centres of two adjacent resonators of the array: 0 is when the receiver is over the first resonator.

where the constants e_1, e_2, e_3, e_4, e_5, e_6, e_7, and e_8 are described in Appendix A.5.

In case we are operating at the resonant frequency (i.e., $\omega = \omega_0$) $\hat{Z}_{eq}$ becomes R_{eq}, and Eqs. (2) and (3) can be written with $\hat{Z} = R$, $\hat{Z}'_T = R'_T$, $\hat{Z}_T = R_T$, $\hat{Z}_d = R_d$ and $\omega = \omega_0$. In [18] an example is shown by applying Eq. (2) repeatedly in order to determine the equivalent impedance of a resonator array loaded with two receivers. In [19] instead, Eq. (2) is used to analyse the conducted emissions generated by a resonator array. In Fig. 2 we can see that the equivalent impedance is affected more significantly as the receiver gets closer to the cell next to the one connected to the source and for higher values of R_d.

3.1. Convergence of the Equivalent Impedance

For the constants a_2 and b_2 given in Appendix A.1, for an infinite number of resonators Eq. (2) converges to the following value:

$$\lim_{n\to\infty} \hat{Z}_{eq} = \frac{1}{2}\left(-\hat{Z} + \sqrt{\hat{Z}^2 + 4\,(\omega M)^2}\right). \tag{4}$$

We can see that Eq. (4) does not depend on the initial conditions, i.e., the impedance $\hat{Z}'_T$. The limit depends only on the electrical parameters of the cells, the mutual inductance M and the angular frequency ω. For example, for a frequency $f = 165\,\text{kHz}$ different than the resonant frequency, we can obtain and plot the equivalent impedance $\hat{Z}_{eq}$ (Fig. 3). For the resonant frequency $f_0 = 147\,\text{kHz}$, the equivalent impedance is shown in Fig. 4. It can be noticed that as we increase the length of the resonator line, even for different values of the impedance $\hat{Z}'_T$ (or resistance R'_T), the equivalent impedance

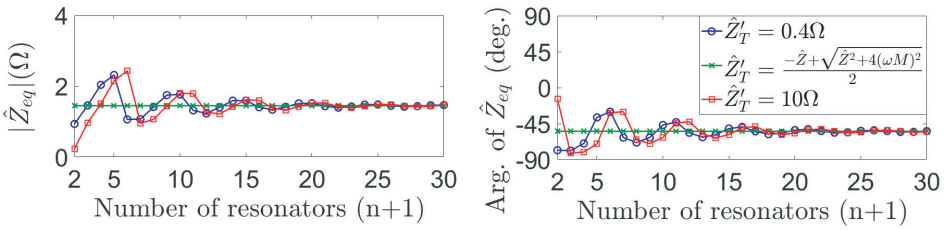

Figure 3. Magnitude and argument of the equivalent impedance $\hat{Z}_{eq}$ versus the number of resonators of the array at $f = 165\text{kHz}$ and for different values of $\hat{Z}'_T$.

converges always to Eq. (4). Furthermore, introducing an impedance $\hat{Z}'_T$ equal to (4) into Eq. (2), the equivalent impedance $\hat{Z}_{eq}$ is constant and equal to $\hat{Z}'_T$ regardless of the number of resonators. Taking Eq. (4) into account, at the resonant frequency the input impedance of the array, i.e., the impedance seen from the source terminals, is

$$R_{in} = R + \frac{1}{2}\left(-R + \sqrt{R^2 + 4\left(\omega_0 M\right)^2}\right) = \frac{1}{2}\left(R + \sqrt{R^2 + 4\left(\omega_0 M\right)^2}\right). \tag{5}$$

Equation (5) coincides with the termination resistance that according to the MIW theory provides matching of the structure [11]. Thus, Eq. (5) can be considered as the characteristic impedance of the line.

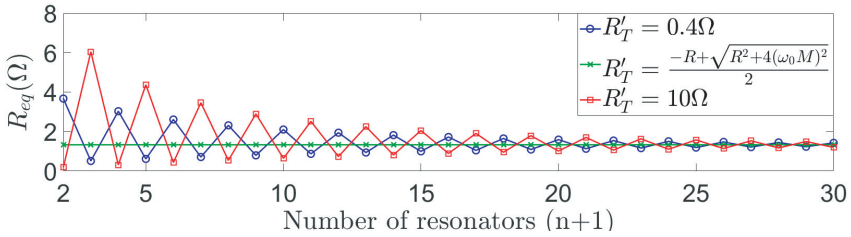

Figure 4. R_{eq} versus the number of resonators of the array at the resonant frequency $f_0 = 147\,\text{kHz}$ and for different values of R'_T.

This also means that when a perturbation $\hat{Z}_d$ is present in the $(j+1)$th resonator, and the line is terminated with an impedance $\hat{Z}'_T$ equal to Eq. (4), we can determine $\hat{Z}_{eq}$ with Eq. (2) by replacing $\hat{Z}'_T$ with $\frac{1}{2}(-\hat{Z} + \sqrt{\hat{Z}^2 + 4(\omega M)^2}) + \hat{Z}_d$ and replacing n with $n - j$.

4. EXPERIMENTAL RESULTS

The theoretical results obtained in this work were verified with the array used in [19], composed of six resonators each formed wrapping 6 turns of stranded wire (section of $3.31\,\text{mm}^2$) around a parallelepiped wooden core of $15\,\text{cm} \times 15\,\text{cm}$ square base. The resonator array is shown in Fig. 5(a). As done in [19], the resonator was supplied by an H-bridge inverter, which uses an FSB44104A Fairchild Semiconductor and is powered by an AIM-TTI Instruments QPX1200SP 1200W DC Power Supply. An Arduino Due microprocessor controls the H-bridge and sets the working frequency equal to the resonant frequency f_0 of the resonators. The first resonator of the array is terminated to a resistive load. An Agilent 4396B 100 kHz–1.8 GHz Vector Network Analyser (VNA) was used to measure the self-inductance, intrinsic AC resistance, added capacitance of the resonators, which were averaged between maximum and minimum values as described in [19] (see Table 1). Note that as the resonators of the array are arranged in a plane, the mutual inductance between each pair of adjacent resonators, determined with the VNA as in [19], is considered negative in Table 1, as done in [11, 13].

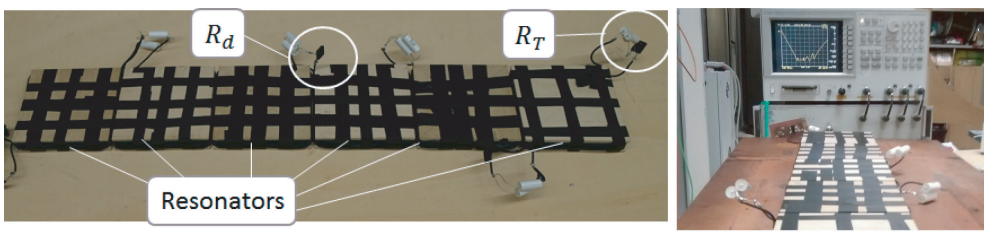

(a) (b)

Figure 5. Experimental setup built in laboratory: (a) array of resonators used for experimental validations, (b) array of resonators connected to a Vector Network Analyser (VNA) for measurements.

Table 1. Average measured circuit parameter values of the resonator array.

Parameter	L (μH)	C (nF)	$R\,(\Omega)$	M (μH)	f_0 (kHz)
Measured values	12.6 ± 0.1	93.1 ± 0.2	0.11 ± 0.01	-1.55 ± 0.05	147.0 ± 0.5

4.1. Input Impedance of the Array with a Receiver over the First Cell (Or with the First Resonator Acting as Receiver) and with a Receiver over the Resonator Line at Any Position

The magnitude of the input impedance of the whole array was measured using the same VNA as shown in Fig. 5(b). Then, the value obtained is compared with the theoretical result given by:

$$\hat{Z}_{in} = \hat{Z} + \hat{Z}_{eq} \tag{6}$$

which can be quickly and easily calculated using Eq. (2) or (3).

The six resonators were used to form five different array configurations, with 2, 3, 4, 5 and 6 resonators. For each configuration, from Eq. (2) with $n = 1, \ldots, 5$, and Eq. (6), we calculate $\hat{Z}_{in}$ at the resonant frequency $f_0 = 147\,\text{kHz}$ for different values of R'_T ($0.4\,\Omega$, $1.5\,\Omega$ and $10\,\Omega$). These results were then compared with the input impedance obtained with the measurements on the same configurations of the system and are shown in Fig. 6. It can be noticed that for $R'_T = 1.5\,\Omega$, Z_{in} tends to the value (5) with much smaller oscillations than for the other two values of R'_T since $R'_T = 1.5\,\Omega$ is the resistance closest to $\frac{1}{2}(-R + \sqrt{R^2 + 4(\omega_0 M)^2}) = 1.38\,\Omega$ which makes the equivalent impedance constant, confirming the theoretical result indicated in Appendix A.4 and Section 3.1. At frequencies different from the resonant one, $\hat{Z}_{in}$ is a complex quantity. As an example, the results are reported in Table 2 for $\hat{Z}'_T = 1.5\,\Omega$.

Figure 6. $\hat{Z}_{in}\,(\Omega)$ at the resonant frequency $f_0 = 147\,\text{kHz}$ obtained with measurements with VNA and with Eq. (6) using Eq. (2) for different values of R'_T ($0.4\,\Omega$, $1.5\,\Omega$ and $10\,\Omega$) and different number of resonators.

Table 2. $\hat{Z}_{in}(\Omega)$ for different frequency values from 135 kHz to 161 kHz obtained with measurements with VNA and with Eq. (6) using Eq. (2) for $\hat{Z}'_T = 1.5\,\Omega$.

f (kHz)	135	140	145	150	155	160
Measurements with VNA	$1.78\angle -55°$	$1.62\angle -22°$	$1.35\angle -2°$	$1.48\angle 19°$	$2.32\angle 24°$	$1.26\angle 36°$
Equation (6)	$1.67\angle -60°$	$1.74\angle -16°$	$1.35\angle -9°$	$1.40\angle 14°$	$1.98\angle 19°$	$1.25\angle 48°$

In case there is a receiver over the ith cell of the resonator array, we can calculate $\hat{Z}_{in}$ in resonance conditions from Eqs. (3) and (6). In the experimental setup, we connected a $5\,\Omega$ resistor to the ith cell to represent the additional impedance R_d. The results are shown in Fig. 7. The small difference between

Figure 7. $\hat{Z}_{in}\,(\Omega)$ at the resonant frequency $f_0 = 147\,\text{kHz}$ obtained with measurement using the VNA and with Eq. (6) using Eq. (3) versus different positions of the receiver.

experiments and calculations comes probably from the imperfections in the manufacturing of the coils, as their self-inductance and resistance can be slightly different. Nevertheless, there is clearly a good agreement between the results, thus validating experimentally the theoretical developments presented in this work and showing their practical applicability to impedance matching.

4.2. Determination of the Input Power Using the Equivalent Impedance

As referred in the introduction of this paper, the value of equivalent impedance could be used, for a given voltage source, to determine the power delivered from the source to a loaded array. Then, assuming that we are working at the resonant frequency, the power delivered from a sinusoidal voltage source with a given RMS value V_s, as represented in Fig. 1 (considering $R_s = 0$), can be given by:

$$P_{in} = \frac{V_s^2}{R_{eq} + R} \tag{7}$$

where R_{eq} is determined with Eq. (2) or with Eq. (3). When a H-bridge resonant inverter is used, the array is fed with a square voltage wave. This means we can set $V_s = V_{s1}$ in q. (7), with V_{s1} determined as in [20]:

$$V_{s1} = \frac{4}{\pi\sqrt{2}} V_{sq} \tag{8}$$

where V_{s1} is the RMS of the fundamental component of the inverter output square wave v_{in}, and V_{sq} is the measured amplitude value of the square wave, whose duty cycle is assumed to be 0.5. Then, through measurements, the input power is obtained as the average value in a period of the product of the instantaneous voltage and current measured at the terminals of the inverter:

$$P_{in,\text{exp}} = \frac{1}{T} \int_0^T v_{in}(t)\, i_{in}(t) \text{dt} \tag{9}$$

where $T = 1/f_0$ is the period of the waveforms, and $v_{in}(t)$ and $i_{in}(t)$ are the measured instantaneous values of the input voltage and current. The product of the instantaneous voltage and current and its average value in a period were calculated with the oscilloscope using the mathematical functions of its internal software. We can then compare the values calculated with the theoretical formula (7) with the experimental ones obtained with Eq. (9). This is done first considering an array of 6 resonators terminated with different values of R'_T ($0.4\,\Omega$, $1.5\,\Omega$, $5\,\Omega$ and $10\,\Omega$) and then an array of 6 resonators terminated with $R'_T = 1.5\,\Omega$ with a receiver in different positions. The results of these two comparisons are presented in Figs. 8 and 9 which show, for a given voltage source, the power P_{in} delivered by the source to a 6-resonator array versus the termination impedance and the receiver position, respectively. Fig. 8 shows that P_{in} increases for an increasing value of R'_T; Fig. 9 shows that for a fixed R'_T, the power delivered by the source has large oscillations depending on the position of the receiver. These examples show some of the possible practical applications of the study of the equivalent impedance on

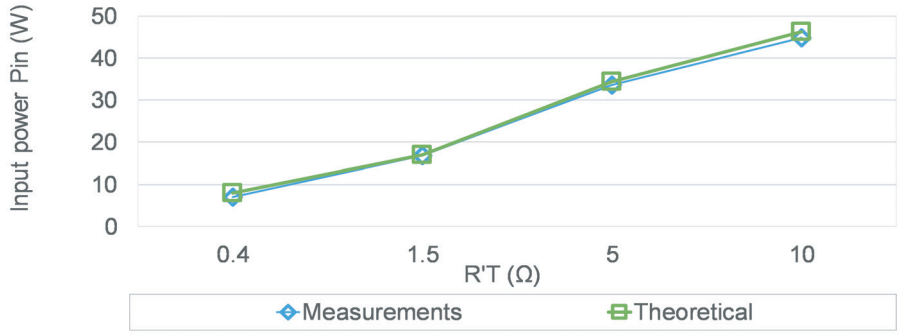

Figure 8. Comparison of $P_{in}(W)$ at the resonant frequency $f_0 = 147\,\text{kHz}$ obtained with measurements using Eq. (9) to the input power calculated through the developed formulae ((7) using $V_s = 4.9\,\text{V}$ determined with Eqs. (8) and (2)) versus R'_T.

Figure 9. Comparison of $P_{in}(W)$ at the resonant frequency $f_0 = 147\,\text{kHz}$ obtained with measurements using Eq. (9) to the input power calculated through the developed formulae ((7) using $V_s = 4.9\,\text{V}$ determined with Eqs. (8) and (3)) versus the position of the receiver.

determining and predicting the input power (and thus the input current) delivered by a given voltage source to the resonator array for different conditions of the system (variable R'_T or variable position of the receiver) which can be useful for the design of the array and its power source.

5. CONCLUSIONS

In this paper, through the application of the theory of linear homogeneous difference equations, an explicit closed-form expression of the equivalent impedance is developed, which depends on the electrical parameters of the resonator array, termination impedance, number of resonators, position and impedance of receivers. Moreover, from the mathematical analysis of the convergence of the recursive sequence that defines the continued fraction, it is found that for an arbitrarily large number of resonators, the equivalent impedance is given only by the electrical parameters of the resonator array, and that it does not depend on the termination impedance and the number of receivers over the line. Furthermore, by terminating the resonator array with the equivalent impedance of an infinite number of resonators, the equivalent impedance of the resonator array is constant for any number of resonators. It is also shown that the recursive sequence used to model the system has an oscillating behaviour.

Then, in order to illustrate the proposed closed-form formulae, some examples of equivalent impedance calculation for different system configurations are provided. Moreover, the theoretical formulae for the equivalent impedance and for the efficiency are validated with experiments, and the comparison shows a very good agreement.

The mathematical approach developed in this work gives a consistent theoretical basis that can be used by electrical engineers not only as a powerful tool for designing resonator arrays for WPT systems with given properties and behaviour, but also more specifically to design the power source that feeds the resonator array and to study the matching of the source with the array. In fact, knowing the array equivalent impedance and its possible variations, the current and active power delivered by a given voltage source can be predicted accurately, thus saving time comparatively to other numerical or simulation software.

ACKNOWLEDGMENT

H. Albuquerque acknowledges financial assistance by the Centre for Mathematics of the University of Coimbra — UID/MAT/00324/2013, funded by the Portuguese Government through FCT/MEC and co-funded by the European Regional Development Fund through the Partnership Agreement PT2020.

APPENDIX A.

A.1. Value of the Fraction without a Perturbation

The continued fraction in Eq. (1) for the particular case where the receiver is over the first cell, can be rewritten using generic letters for any number $n+1$ of resonators (with $n \geq 0$):

$$x_n = \cfrac{a}{b + \cfrac{a}{\cdots + \cfrac{a}{b + \cfrac{p_0}{q_0}}}} \tag{A1}$$

with a, b, p_0, $q_0 \in \mathbb{C}$ where $q_0 \neq 0$, a and b both not equal to 0, and in case $a \neq 0$ then $p_0 \neq 0$. The previous fraction in Eq. (A1) is the nth term of the following recursive sequence (with $k \geq 1$):

$$x_k = \frac{a}{b + x_{k-1}}, \text{ with } x_0 = \frac{p_0}{q_0}. \tag{A2}$$

The term x_0 corresponds to the termination impedance of the first cell, e.g., $\hat{Z}'_T$ or $\hat{Z}_T$ in Eq. (1). In this way, labelling the $n+1$ cells of the array from 1 to $n+1$, 1 is the first array cell and $n+1$ is the cell connected to the source. Thus, noting by

$$x_k = \frac{p_k}{q_k}, \tag{A3}$$

we verify by induction that $\{p_n\}$ and $\{q_n\}$ are sequences defined by the following recurrence relations:

$$\begin{matrix} p_n = bp_{n-1} + ap_{n-2} \\ q_n = bq_{n-1} + aq_{n-2} \end{matrix} \text{ for } n \geq 2, \tag{A4}$$

being p_0 and q_0 fixed and

$$\begin{matrix} p_1 = aq_0 \\ q_1 = bq_0 + p_0 \end{matrix}. \tag{A5}$$

Equation (A4) of the type $p_n - bp_{n-1} - ap_{n-2} = 0$ is a linear homogeneous second order difference equation with constant coefficients and its solution is given by $p_n = m_1\lambda_1^n + m_2\lambda_2^n$ supposing that λ_1 and λ_2 are distinct solutions of the equation $\lambda^2 - b\lambda - a = 0$:

$$\lambda_1 = \frac{b - \sqrt{b^2 + 4a}}{2}; \quad \lambda_2 = \frac{b + \sqrt{b^2 + 4a}}{2} \tag{A6}$$

in which m_1 and m_2 are constants that should be determined using the initial conditions. Analogous considerations can be done for $\{q_n\}$.

Concluding, the general term of the sequence $\{x_n\} = \frac{\{p_n\}}{\{q_n\}}$ is given by

$$x_n = \frac{a_1\left(\frac{b-\sqrt{b^2+4a}}{2}\right)^n + a_2\left(\frac{b+\sqrt{b^2+4a}}{2}\right)^n}{b_1\left(\frac{b-\sqrt{b^2+4a}}{2}\right)^n + b_2\left(\frac{b+\sqrt{b^2+4a}}{2}\right)^n} \tag{A7}$$

where a_1, a_2, b_1 and b_2 are determined by the initial conditions x_0 and x_1, and are given in Eq. (A.3), assuming, for simplicity that $p_0 = x_0$ and $q_0 = 1$.

A.2. Value of the Fraction with a Perturbation in the *i*th Term

We determine now the value of expression (1), which is the equivalent impedance of a multiple resonator system for a receiver placed over the ith cell of the receiver line. To do this, we rewrite the fraction as a generic continued fraction of the nth order with a perturbation $b' \neq b$ in the step $i \leq n$ of the recursive sequence:

$$x_n = \cfrac{a}{b+\cfrac{a}{\ldots+\cfrac{a}{b'+\cfrac{a}{b+\cfrac{a}{\ldots+\cfrac{a}{b+\frac{p_0}{q_0}}}}}}} \quad \text{with } a,\ b,\ b',\ p_0,\ q_0 \in \mathbb{C}. \tag{A8}$$

To solve this fraction, we split the fraction in two continued fractions (one with i and the other with $n-i$ terms). After calculating the value of x_k for the $(i-1)$th term, we determine the ith value x_i using the perturbation b' and, finally, using x_i as an initial value, we compute the value of the fraction, with the last $n-i$ values. So, we start using Eq. (A7) to determine the term of $(i-1)$th order:

$$x_{i-1} = \frac{a_1\left(b-\sqrt{b^2+4a}\right)^{i-1} + a_2\left(b+\sqrt{b^2+4a}\right)^{i-1}}{b_1\left(b-\sqrt{b^2+4a}\right)^{i-1} + b_2\left(b+\sqrt{b^2+4a}\right)^{i-1}} \tag{A9}$$

where a_1, a_2, b_1 and b_2 are determined by the initial conditions x_0 and x_1 as done before in Eq. A.1. After, we have to calculate the value of

$$x_i = \frac{a}{b'+x_{i-1}} = y_0; \text{ and } \frac{a}{b+y_0} = y_1. \tag{A10}$$

Then, Eqs. (A10) are the initial conditions used to determine the value of the fraction $y_{n-i} = x_n$:

$$y_{n-i} = \frac{c_1\left(b-\sqrt{b^2+4a}\right)^{n-i} + c_2\left(b+\sqrt{b^2+4a}\right)^{n-i}}{d_1\left(b-\sqrt{b^2+4a}\right)^{n-i} + d_2\left(b+\sqrt{b^2+4a}\right)^{n-i}}. \tag{A11}$$

The constants c_1, c_2, d_1 and d_2 are computed using the initial conditions y_0 and where it is assumed that $p_0 = y_0$ and $q_0 = 1$. These constants are given in A.3

Expression (A11) represents the value of the fraction in Eq. (1) for $n+1$ resonators with the perturbation in the ith term, (receiver facing the ith resonator, i.e., $i = 1$ corresponds to the first resonator and $i = n$ to the resonator next to the one connected to the source).

A.3. Constants a_1, a_2, b_1, b_2, c_1, c_2, d_1, d_2

$$a_1 = \frac{x_0}{2} - \frac{2a - bx_0}{2\sqrt{b^2+4a}};\ a_2 = \frac{x_0}{2} + \frac{2a - bx_0}{2\sqrt{b^2+4a}};\ b_1 = \frac{1}{2} - \frac{2x_0 + b}{2\sqrt{b^2+4a}};\ b_2 = \frac{1}{2} + \frac{2x_0 + b}{2\sqrt{b^2+4a}};$$
$$c_1 = \frac{y_0}{2} - \frac{2a - y_0 b}{2\sqrt{b^2+4a}};\ c_2 = \frac{y_0}{2} + \frac{2a - y_0 b}{2\sqrt{b^2+4a}};\ d_1 = \frac{1}{2} - \frac{2y_0 + b}{2\sqrt{b^2+4a}};\ d_2 = \frac{1}{2} + \frac{2y_0 + b}{2\sqrt{b^2+4a}}.$$

A.4. Convergence of the Continued Fraction

Following the study of the fraction, we can predict its behaviour for an infinite number of terms, in other words, its value for $n \to \infty$.

Supposing that $z^2 - bz - a = 0$ has distinct roots $z_1 = b + \sqrt{b^2+4a}$ and $z_2 = b - \sqrt{b^2+4a}$, with $|z_1| > |z_2|$, we have

$$\left|\frac{z_2}{z_1}\right| < 1,\ \text{so}\ \lim_{n\to\infty}\left(\frac{z_2}{z_1}\right)^n = 0. \tag{A12}$$

and

$$x_n = \frac{a_2 z_1^n + a_1 z_2^n}{b_2 z_1^n + b_1 z_2^n},\ \text{thus}\ \lim_{n\to\infty} x_n = \lim_{n\to\infty} \frac{a_2 + a_1\left(\frac{z_2}{z_1}\right)^n}{b_2 + b_1\left(\frac{z_2}{z_1}\right)^n} = \frac{a_2}{b_2}. \tag{A13}$$

This proves a very important fact: for fixed a, $b \in \mathbb{C}$, the value of the fraction is the same, $a_2/b_2 = \frac{1}{2}(\sqrt{4a+b^2} - b)$ when the number of terms is infinite, not depending of the initial condition x_0. So if we take x_0 equal to this value $\{x_n\}$ becomes a constant sequence. Moreover, for a finite number of perturbations, the behaviour of the fraction at infinity remains the same.

A.5. Determination of the Constants of the Fraction

$$e_1 = \hat{Z}_d\left(2(\omega M)^2 - f\hat{Z}_T\right);\ e_2 = \hat{Z}_d\left(2(\omega M)^2 - g\hat{Z}_T\right)$$
$$e_3 = g\left(\hat{Z} - \hat{Z}_d\right)\hat{Z}_T + 2(\omega M)^2\left(-h + \hat{Z}_d + 2\hat{Z}_T\right)$$
$$e_4 = f\left(\hat{Z} - \hat{Z}_d\right)\hat{Z}_T + 2(\omega M)^2\left(h + \hat{Z}_d + 2\hat{Z}_T\right)$$
$$e_5 = (\omega M)^2\left(4(\omega M)^2 + f\left(\hat{Z} + \hat{Z}_d\right) + 2\left(-h + \hat{Z}_d\right)\hat{Z}_T\right)$$
$$e_6 = \hat{Z}_d\left(f\hat{Z}\hat{Z}_T + (\omega M)^2\left(-f + 2\hat{Z}_T\right)\right);\ e_7 = \hat{Z}_d\left(g\hat{Z}\hat{Z}_T - (\omega M)^2\left(g - 2\hat{Z}_T\right)\right)$$
$$e_8 = (\omega M)^2\left(4(\omega M)^2 + g\left(\hat{Z} + \hat{Z}_d\right) + 2\left(h + \hat{Z}_d\right)\hat{Z}_T\right)$$

Note: for resonance conditions $\hat{Z}$, $\hat{Z}_T$ and $\hat{Z}_d$ are replaced by R, R_T and R_d, respectively.

REFERENCES

1. Olvitz, L., D. Vinko, and T. Svedek, "Wireless power transfer for mobile phone charging device," *Proc. 35th Int. Convention MIPRO 2012*, 141–145, May 2012.
2. Nguyen, M. Q., Z. Hughes, P. Woods, Y. S. Seo, S. Rao, and J. C. Chiao, "Field distribution models of spiral coil for misalignment analysis in wireless power transfer systems," *IEEE Trans. on Microwave Theory and Techniques*, Vol. 62, No. 4, 920–930, Apr. 2014.
3. Li, S. and C. C. Mi, "Wireless power transfer for electric vehicle applications," *IEEE Journal of Emerging and Selected Topics in Power Electronics*, Vol. 3, No. 1, 4–17, Mar. 2015.

4. Kamineni, A., G. A. Covic, and J. T. Boys, "Analysis of coplanar intermediate coil structures in inductive power transfer systems," *IEEE Trans. on Power Electronics*, Vol. 30, No. 11, 6141–6154, Nov. 2015
5. Zhong, W., C. K. Lee, and S. Y. R. Hui, "General analysis on the use of Tesla's resonators in domino forms for wireless power transfer," *IEEE Trans. on Industrial Electronics*, Vol. 60, No. 1, 261–270, Jan. 2013.
6. Wang, B., W. Yerazunis, and K. H. Teo, "Wireless power transfer: Metamaterials and array of coupled resonators," *Proceedings of the IEEE*, Vol. 101, No. 6, 1359–1368, Jun. 2013.
7. Hui, S. Y. R., W. Zhong, and C. K. Lee, "A critical review of recent progress in mid-range wireless power transfer," *IEEE Trans. on Power Electronics*, Vol. 29, No. 9, 4500–4511, Sept. 2014.
8. Alberto, J., G. Puccetti, G. Grandi, U. Reggiani, and L. Sandrolini, "Experimental study on the termination impedance effects of a resonator array for inductive power transfer in the hundred kHz range," *Proc. 2015 IEEE Wireless Power Transfer Conference (WPTC 2015)*, 1–4, Boulder, CO, USA, May 2015.
9. Monti, G., L. Corchia, L. Tarricone, and M. Mongiardo, "A network approach for wireless resonant energy links using relay resonators," *IEEE Trans. on Microwave Theory and Techniques*, Vol. 64, No. 10, 3271–3279, Oct. 2016.
10. Moon, S. and G. W. Moon, "Wireless power transfer system with an asymmetric four-coil resonator for electric vehicle battery chargers," *IEEE Trans. on Power Electronics*, Vol. 31, No. 10, 6844–6854, Oct. 2016.
11. Stevens, C. J., "Magnetoinductive waves and wireless power transfer," *IEEE Trans. on Power Electronics*, Vol. 30, No. 11, 6182–6190, Nov. 2015.
12. Syms, R. R. A., I. R. Young, and L. Solymar, "Low-loss magneto-inductive waveguides," *Journal of Physics D: Applied Physics*, Vol. 39, No. 18, 3945, 2006.
13. Puccetti, G., C. J. Stevens, U. Reggiani, and L. Sandrolini, "Experimental and numerical investigation of termination impedance effects in wireless power transfer via metamaterial," *Energies*, Vol. 8, No. 3, 1882–1895, 2015.
14. Beato-Lopez, J., C. de la Cruz Blas, A. Mitra, and C. Gomez-Polo, "Electrical model of giant magnetoimpedance sensors based on continued fractions," *Sensors and Actuators A: Physical*, Vol. 242, 73–78, 2016.
15. Gong, Z., Z. Tang, S. Mukamel, J. Cao, and J. Wu, "A continued fraction resummation form of bath relaxation effect in the spin-boson model," *The Journal of Chemical Physics*, Vol. 142, No. 8, 084103, 2015.
16. Puccetti, G., U. Reggiani, and L. Sandrolini, "Experimental analysis of wireless power transmission with spiral resonators," *Energies*, Vol. 6, No. 11, 5887–5896, 2013.
17. Elaydi, S., *An Introduction to Difference Equations*, Springer Science & Business Media, 2005.
18. Alberto, J., U. Reggiani, and L. Sandrolini, "Circuit model of a resonator array for a WPT system by means of a continued fraction," *Proc. 2016 IEEE 2nd Int. Forum on Research and Technologies for Society and Industry Leveraging a Better Tomorrow (RTSI)*, 1–6, Bologna, Italy, Sept. 2016.
19. Alberto, J., U. Reggiani, and L. Sandrolini, "Study of the conducted emissions of an IPT system composed of an array of magnetically coupled resonators," *Proc. 2017 IEEE Int. Symposium on Electromagn. Compat. Signal/Power Integrity (EMCSI)*, 623–628, Washington, DC, USA, Aug. 2017.
20. Kazimierczuk, M. K., "Class D voltage-switching MOSFET power amplifier," *IEE Proceedings B-Electric Power Applications*, Vol. 138, No. 6, 285–296, IET, 1991.